Netherlands
organization for
applied scientific
research

TNO-report

TNO Physics and Electronics
Laboratory

P O. Box 96864
250[illegible]
Oud[illegible]
The[illegible]
Fax[illegible]
Phone +31 70 326 42 21

report no. FEL-91-A305 — copy no. 8

title

Pattern synthesis for unequally-spaced array antennas with non-identical elements

author(s):

Dr. ir. H.J. Stam

date :

November 1991

classification

title	: unclassified
abstract	: unclassified
report text	: unclassified
appendix A to C	: unclassified

no. of copies	: 25
no. of pages	: 39 (incl. appendices, excl. RDP & distribution list)
appendices	: 3

All information which is classified according to Dutch regulations shall be treated by the recipient in the same way as classified information of corresponding value in his own country. No part of this information will be disclosed to any party.

report no.	:	FEL-91-A305
title	:	Pattern synthesis for unequally-spaced array antennas with non-identical elements
author(s)	:	Dr. ir. H.J. Stam
institute	:	TNO Physics and Electronics Laboratory
date	:	November 1991
NDRO no.	:	A91KM636
no. in pow '91	:	710.2
Research supervised by:		Ir. J.G. van Hezewijk
Research carried out by:		Dr. ir. H.J. Stam

ABSTRACT (UNCLASSIFIED)

A novel method of array antenna pattern synthesis is presented that is based on an optimization technique. The complex excitation values of the current distribution of the array elements are taken as parameters. The radiated far field pattern is matched to one that is prescribed by minimizing a global mean square error. The method is suitable for general arrays like linear, planar and conformal ones, and does not require the factorization into an element factor and an array factor. In contrast with Fourier-like methods the array elements may be arbitrarily placed. Although the theory is developed for arrays of identical elements, it applies to the case of arrays containing non-identical elements as well. Numerical results are presented for unequally-spaced planar arrays of short electric dipoles.

rapport no. : FEL-91-A305

titel : Patroonsynthese voor een array antenne met niet-identieke willekeurig geplaatste elementen

auteur(s) : dr. ir. H.J. Stam

instituut : Fysisch en Elektronisch Laboratorium TNO

datum : november 1991

hdo-opdr.no. : A91KM636

no. in iwp '91 : 710.2

Onderzoek uitgevoerd o.l.v. : Ir. J.G. van Hezewijk

Onderzoek uitgevoerd door : Dr. ir. H.J. Stam

SAMENVATTING (ONGERUBRICEERD)

Een nieuwe methode voor array antenne patroonsynthese wordt gepresenteerd, die gebaseerd is op een optimaliseringstechniek. De complexe excitatie-coefficiënten van de array elementen zijn de ontwerp parameters. Het gewenste verre veld antennepatroon wordt zo goed mogelijk benaderd op basis het minimaliseren van een gemiddelde kwadratische fout.

De methode is geschikt voor zowel lineaire, vlakke als niet-vlakke arrays en kent geen uitsplitsing van het verre veld patroon in een element en array factor. In tegenstelling tot Fourier-achtige methoden mogen de antenne-elementen willekeurig geplaatst worden. Hoewel de theorie is opgezet voor arrays van identieke elementen is de theorie ook bruikbaar voor niet-identieke elementen. Numerieke resultaten worden getoond voor een vlakke array antenne van niet-equidistante elektrische dipolen.

1 INTRODUCTION

In array antenna synthesis problems an optimum choice of the design parameters is aimed at such that the radiation pattern of the array approximates in a certain sense a desired one. As the design parameters for an array antenna there are available the number of elements, their orientations and positions and the amplitudes and phases of their excitations. The desired radiation pattern is either partly fixed by one or more of its characteristics like the directive gain, the beamwidth, the sidelobe level or directions in which zero power has to be radiated (null directions) [1]-[6], or specified in all observational directions by prescribing a complete radiation pattern. In the latter case we are dealing with pattern matching.

The different methods of pattern matching can be distinguished by the manner in which they model the synthesis problem. First, there are the sampling methods where the design parameters of the array antenna are chosen to match (exactly or within some tolerance) the prescribed pattern in a discrete number of directions of radiation [7]-[9]. Next, there are many methods that model the matching problem as a minimization problem. In this case the design parameters are chosen to minimize some error within the concept of a given error criterion. Commonly used error criteria in this respect are the minimax error [10]-[13] and the mean square error [4],[14]-[16]. Recently, methods have been developed that model the matching problem as an intersection problem in the space of admissible radiation patterns [17]-[19]. Each requirement of the radiation pattern that is to be synthesized leads to the admissibility of a subset in the set of all the realizable radiation patterns. A radiation pattern that is an element of the intersection of all these subsets meets all the requirements stated and is looked for.

Many of the array synthesis methods apply to equispaced linear or planar arrays. However, unequally-spaced arrays are also of great interest [13]-[15], [20]-[27]. In case the array is to be used as a directional antenna with high resolution rather than high gain, unequally-spaced arrays will often be superior to equispaced arrays. The unequally-spaced arrays require fewer elements to produce a certain resolution, and their main beam can be steered over a larger frequency bandwidth than is the case with an equispaced array. Arrays with variable interelement spacings can approximate a radiation pattern more closely than arrays with constant spacings because of the extra degree of freedom that is introduced by the variability of the spacings.

In most methods known for unequally-spaced arrays the complex excitations of the elements of the array are fixed and their relative positions are taken as the design parameters [20]-[27]. Once these positions have been fixed it may be advantageous to perform a second step in the synthesis procedure by considering the complex excitations as the design parameters and apply a method to find the optimum values of the latter in order to further improve the approximation to the prescribed radiation pattern. So, in this case we need a synthesis method that performs a pattern matching given the positions of the fixed, unequally-spaced array elements. For unequally-spaced linear arrays such a method has been described in [13]. For unequally-spaced planar arrays the iterative sampling method [8,9] or the computational methods described in [15] are suitable. A disadvantage of the iterative sampling method is that there is no guarantee of the existence of a solution. In case a solution is found, this need not be an optimum one in any sense. Thus, better solutions may exist that are not found by this method. The method described in [15] does not have these difficulties since it is based on the minimization of an error function. It provides an unique optimum solution. However, that theory has only been applied to point sources that are arbitrarily distributed in a plane and to a pattern synthesis within that plane. In addition, the error function is based on the deviations of the synthesized radiation pattern from the prescribed one at a finite set of discrete points of observation. There is no control of the radiation field at the points in between.

In this paper, a pattern synthesis method is presented for unequally-spaced array antennas that may consist of non-identical elements. It involves the minimization of the quadratic error integrated over the unit sphere on which the far-field radiation pattern is defined, and applies to the (transverse) electric field radiation characteristic defined on that sphere. Since the (transverse) magnetic field radiation characteristic is identical to the one for the electric field, the mismatch in the magnetic field is simultaneously minimized with the mismatch in the electric field. The class of admissible patterns that may be prescribed is chosen in accordance with the physics of the electromagnetic radiation of the array elements.

The analysis is carried out in the frequency domain (ω-domain) and considers arrays consisting of arbitrarily oriented, possibly different, elements (electric dipoles, radiating apertures). The action of each element is characterized by a properly normalized spatial distribution function of volume or surface current, and a complex excitation coefficient that determines the amplitude and phase impressed on this distribution. The excitation coefficients are the "design parameters" of the synthesis problem. It is assumed that they can be chosen independently, i.e., mutual coupling is neglected. The radiation field of the array antenna follows by the summation of the fields generated by the individual elements. In this representation, the complex excitation coefficients occur as expansion coefficients. Next, the representation is substituted into the error criterion and a variational method is applied to minimize it. This leads to a system of equations the solution of which provides the optimum choices of the complex excitation coefficients.

The theory is more general than for the case of identical elements which is usually considered and where a factorization into an element factor and an array factor is carried through. The more general case that we consider admits no such factorization. (Note that the removal of this restriction yields an extra degree of freedom in the design of the antenna.)
The array antenna is assumed to be present in free space. Numerical results are presented for different planar arrays. The analysis is organized such that a number of steps can be carried out analytically, which leads to a saving in computation time.

2 BASIC EQUATIONS AND SOURCE-TYPE REPRESENTATIONS FOR THE ELECTRIC AND THE MAGNETIC FIELD STRENGTHS

The array antenna is present in free space having electromagnetic medium properties given by the permittivity ε_0 and the permeability μ_0. To specify the position in the configuration we employ the standard coordinates $\{x_1,x_2,x_3\}$ with respect to a fixed, orthogonal, Cartesian reference frame with origin O (the phase center of the array antenna) and the three mutually perpendicular base vectors $\{i_1,i_2,i_3\}$ of unit length each. In the indicated order the base vectors form a right-handed system. The subscript notation for Cartesian vectors and tensors is employed and the summation convention applies. The corresponding lower-case subscripts are to be assigned the values 1,2,3. This usage leads to expressions that are effortlessly translated into the statements of a computer program written in some high-level programming language. Partial differentiation is denoted by ∂; ∂_p denotes differentiation with respect to x_p.
The analysis is performed in the frequency domain (ω-domain). The complex time factor is $\exp(j\omega t)$, where t is the time coordinate and j^2=-1. The electromagnetic wave field generated by the array antenna is represented by the electric field strength E_k and the magnetic field strength H_j and the volume source densities by J_k and K_j. The corresponding Maxwell equations are [28, p.3]

$$-\varepsilon_{kmp}\,\partial_m H_p + j\omega\varepsilon_0 E_k = -J_k, \tag{1}$$

$$\varepsilon_{jmr}\,\partial_m E_r + j\omega\mu_0 H_j = -K_j, \tag{2}$$

where ε_{kmp} is the completely anti-symmetric unit tensor of rank three (Levi-Civita tensor) defined by

$$\varepsilon_{kmp} = \begin{cases} -1 & \text{when } \{k,m,p\} \text{ is an odd permutation of } \{1,2,3\}, \\ 0 & \text{when not all subscripts are different,} \\ 1 & \text{when } \{k,m,p\} \text{ is an even permutation of } \{1,2,3\}. \end{cases} \tag{3}$$

Equations (1) and (2) govern the propagation of the electromagnetic waves in free space generated by the source distributions J_k and K_j.

The frequency-domain source-type representations for the electric and the magnetic field strengths of the field radiated by distributed sources present in the bounded source domain D^T are given by ([28, p.38])

$$E_k = -j\omega\mu_0 A_k + (j\omega\varepsilon_0)^{-1}\partial_k\partial_r A_r - \varepsilon_{kmp}\partial_m F_p, \tag{4}$$

and

$$H_j = -j\omega\varepsilon_0 F_j + (j\omega\mu_0)^{-1}\partial_j\partial_p F_p + \varepsilon_{jmr}\partial_m A_r, \tag{5}$$

in which

$$A_k(x,\omega) = \int_{x' \in D^T} G(x-x',\omega)J_k(x',\omega)\mathrm{d}V \tag{6}$$

is the electric source current vector potential and

$$F_j(x,\omega) = \int_{x' \in D^T} G(x-x',\omega)K_j(x',\omega)\mathrm{d}V \tag{7}$$

is the magnetic source current vector potential. Here,

$$G(x,\omega) = \exp(-jk_0|x|)/4\pi|x|, \tag{8}$$

is the scalar free-space Green's function (point-source solution) with

$$k_0 = \omega(\mu_0\varepsilon_0)^{1/2} = \omega/c_0 = 2\pi/\lambda_0, \tag{9}$$

where c_0 is the electromagnetic wavespeed in vacuum and λ_0 is the free space wavelength. In our pattern synthesis problem we are only interested in the radiation field in the far-field region for which the far-field parts provide the relevant expressions. In these expressions the following approximations are used: (Collin and Zucker 1969, p.140)

$$|\mathrm{x}-\mathrm{x}'| \approx |\mathrm{x}| - \xi_s x_s' + \text{vanishing terms as } |\mathrm{x}| \to \infty \tag{9a}$$

in the exponential function occurring in the Green's function, where

$$\xi_s = x_s/|\mathbf{x}| \tag{9b}$$

is the unit vector in the direction of observation, and

$$|\mathbf{x}-\mathbf{x}'| \approx |\mathbf{x}|, \tag{9c}$$

in each denominator of the expression for the far-field part. The far-field approximation follows as ([28], p.39])

$$\{E_k,H_j\}(x,\omega) \approx \{E_k^\infty,H_j^\infty\}(\underline{\xi},\omega)\exp(-jk_0|x|)/4\pi|x| \text{ as } |x|'\infty, \tag{10}$$

in which $\underline{\xi}=x/|x|$ is the unit vector in the direction of observation,

$$E_k^\infty = -j\omega\mu_0(\delta_{kr}-\xi_k\xi_r)A_r^\infty + jk_0\varepsilon_{kmp}\xi_m F_p^\infty \tag{11}$$

and

$$H_j^\infty = -j\omega\varepsilon_0(\delta_{jp}-\xi_j\xi_p)F_p^\infty - jk_0\varepsilon_{jmr}\xi_m A_r^\infty, \tag{12}$$

where

$$\{A_r^\infty,F_p^\infty\}(\underline{\xi},\omega) = \int_{x'\in D^T} \{J_r,K_p\}(x',\omega)\exp(jk_0\xi_s x_s')\mathrm{d}V, \tag{13}$$

are the far-field radiation characteristics of the current distribution.

As (10) shows, the electric and the magnetic field strength have, in the far-field region, the structure of a spherical wave that expands radially from the origin of the coordinate system (which is also denoted as the phase center of the far-field approximation), the latter being chosen in the neighbourhood of the radiating sources, with an amplitude that depends on the direction of observation and that decreases inversely proportional to the distance from the sources. The amplitude radiation characteristics $\{E_k^\infty,H_j^\infty\}$ depend only on the direction of observation $\underline{\xi}$, and on ω.

The far-field amplitude radiation characteristics E_k^∞ and H_j^∞ of the electric and the magnetic field strengths are not independent of each other. It is easily verified that the right-hand sides of (11) and (12) are interrelated in the following way: (De Hoop 1990, p 10-27)

$$\varepsilon_{kmp}\xi_m H_p^{\infty} + YE_k^{\infty} = 0, \tag{14}$$

$$-\varepsilon_{jmr}\xi_m E_r^{\infty} + ZH_j^{\infty} = 0, \tag{15}$$

in which

$$Y = (\varepsilon_0/\mu_0)^{1/2} \text{ and } Z = (\mu_0/\varepsilon_0)^{1/2} \tag{16}$$

are the plane-wave admittance and impedance of free space, respectively. Note that

$$\xi_k E_k^{\infty} = 0 \text{ and } \xi_j H_j^{\infty} = 0, \tag{17}$$

i.e., in the far-field region the electric and the magnetic field strengths are transverse with respect to the local radial direction of propagation $\underline{\xi}$ of the wave, and are, since ε_{kmp} and ξ_m have unit magnitudes, proportional with proportionality factors Y and Z. The directive gain (or directivity) of the antenna array [28, p.33] is

$$\begin{aligned} D(\underline{\xi},\omega) &= \frac{4\pi E_j^{\infty}(\underline{\xi},\omega)E_j^{*\infty}(\underline{\xi},\omega)}{\int_{\underline{\xi}'\in\Omega} E_j^{\infty}(\underline{\xi}',\omega)E_j^{*\infty}(\underline{\xi}',\omega)\mathrm{d}\Omega} \\ &= \frac{4\pi H_j^{\infty}(\underline{\xi},\omega)H_j^{*\infty}(\underline{\xi},\omega)}{\int_{\underline{\xi}'\in\Omega} H_j^{\infty}(\underline{\xi}',\omega)H_j^{*\infty}(\underline{\xi}',\omega)\mathrm{d}\Omega} \quad \text{for } \underline{\xi}\in\Omega, \end{aligned} \tag{18}$$

where Ω is the unit sphere around the phase center of the antenna.

3 OPTIMIZATION TECHNIQUES IN ARRAY ANTENNA PATTERN SYNTHESIS

3.1 Introduction

In this section, the optimization technique will be developed for elements with electr' current volume source distributions and for a prescribed radiation characteristic of the electric field strength within the class of vector functions that are tangential to the unit sphere. The technique for other types of elements (such as radiating apertures) goes along the same lines, while in view of the equality of the (transverse) electric and magnetic field radiation characteristics, the minimization of the mismatch in electric field simultaneously minimizes the mismatch of the corresponding magnetic field. The volume source current differs from zero in a given bounded domain D^T; D^T is the union of the domains $\{D^T(I); I=1,...,N\}$ occupied by the separate elements (N = number of elements).

3.2 The Pattern Synthesis Problem formulated as a Minimization Problem

To arrive at the error criterion that will be minimized in our synthesis problem, we first introduce the inner product $<.,.>_\Omega$ defined on the unit sphere Ω. For two vector functions $P(\underline{\xi},\omega)$ and $Q(\underline{\xi},\omega)$ this inner product is taken as

$$<P,Q>_\Omega = \int_{\underline{\xi}\in\Omega} w(\underline{\xi}) P_p(\underline{\xi},\omega) Q_p^*(\underline{\xi},\omega)\,d\Omega, \qquad (19)$$

where Ω is the unit sphere around the origin and $w(\underline{\xi})$ is a real positive weighting function ($w(\underline{\xi})>0$ for all $\underline{\xi}$) and * denotes complex conjugate. The global error function that describes the mismatch between the prescribed radiation characteristic $E^{D\infty}=E^{D\infty}(\underline{\xi},\omega)$ and the radiation characteristic E^∞ realized by the array is chosen as

$$\mathrm{ERR}(E^\infty) = \|E^\infty - E^{D\infty}\|_\Omega = (<E^\infty-E^{D\infty},E^\infty-E^{D\infty}>_\Omega)^{1/2}. \qquad (20)$$

The weighting function occurring in the definition of this norm (cf. 19) provides the possibility to match the radiation pattern of the antenna in some directional area better than in other directional areas.

For the class of elements under consideration, we have in view of (11)

$$E_k^\infty = -j\omega\mu_0(\delta_{kr}-\xi_k\xi_r)A_r^\infty, \tag{21}$$

where A_r^∞ is given by (cf. (13)):

$$A_r^\infty(\underline{\underline{\xi}},\omega) = \int_{x\in D^T} J_r(x,\omega)\exp(jk_0\xi_s x_s)\mathrm{d}V. \tag{22}$$

Note that the integration variable x' has been replaced by x.

Let $j(x,\omega;I)$ be the normalized source distribution of the element occupying the domain $D^T(I)$ ($I=1,\ldots,N$), and let $c(\omega;I)$ be its complex excitation coefficient, then

$$A_r^\infty(\underline{\underline{\xi}},\omega) = \sum_{I=1}^{N} c(\omega;I)a_r^\infty(\underline{\underline{\xi}},\omega;I) \tag{23}$$

with

$$a_r^\infty(\underline{\underline{\xi}},\omega;I) = \int_{x\in D^T(I)} j_r(x,\omega;I)\exp(jk_0\xi_s x_s)\mathrm{d}V, \quad \text{for } I=1,\ldots,N, \tag{24}$$

and

$$E_k^\infty(\underline{\underline{\xi}},\omega) = \sum_{I=1}^{N} c(\omega;I)e_k^\infty(\underline{\underline{\xi}},\omega;I) \tag{25}$$

with

$$e_k^{\infty}(\underline{\xi},\omega;I) = -j\omega\mu_0(\delta_{kr}-\xi_k\xi_r)a_r^{\infty}(\underline{\xi},\omega;I) \qquad \text{for } I=1,\dots,N. \tag{26}$$

Substitution of the expansion (25) into (20) gives for the squared norm of the mismatch in the field

$$\begin{aligned}\|E^{\infty}-E^{D\infty}\|^2{}_{\Omega} = {} & \|E^{D\infty}\|^2{}_{\Omega} - 2\mathrm{Re}[\sum_{I=1}^{N} c^{*}(\omega;I)<E^{D\infty}(\underline{\xi},\omega),e^{\infty}(\underline{\xi},\omega;I)>] \\ & + \sum_{I=1}^{N}\sum_{J=1}^{N} c(\omega;I)c^{*}(\omega;J)<e^{\infty}(\underline{\xi},\omega;I),e^{\infty}(\underline{\xi},\omega;J)>.\end{aligned} \tag{27}$$

To arrive at the condition for the optimum complex excitation coefficients $c^{opt}(\omega;I)$, $I,\dots,N$, that minimize the squared error (27), we apply a variational analysis. As a result, the following system of equations is obtained (see Appendix A):

$$\sum_{I=1}^{N} c^{opt}(\omega;I)<e^{\infty}(\underline{\xi},\omega;I),e^{\infty}(\underline{\xi},\omega;J)> = \; <E^{D\infty}(\underline{\xi},\omega),e^{\infty}(\underline{\xi},\omega;J)> \qquad \text{for } J=1,\dots,N. \tag{28}$$

Given an array antenna for which the electric current volume source distributions of its elements, and hence the functions $j(x,\omega;I)$, $I=1,\dots,N$, are known, the matrix elements of the system matrix in (28) follow from (24) and (26). Together with the specification of the right-hand side through the desired pattern $E^{D\infty}$, the system of equations (28) is completely known and can be solved for the optimum excitations $c^{opt}(\omega;I)$, $I=1,\dots,N$. The prescribed radiation characteristic of the electric field strength is taken from the class of vector functions that are tangential to the unit sphere (cf. (21)), i.e.,

$$E_k^{D\infty} = \; -j\omega\mu_0(\delta_{kr}-\xi_k\xi_r)\mathrm{A}_r^{D\infty}, \tag{29}$$

where $\mathrm{A}_r^{D\infty}$ is user prescribed. In fact, we prescribe the far-field radiation characteristic of the electric current distribution $\mathrm{A}_r^{D\infty}$ from which $E_k^{D\infty}$ follows that is to be approximated by E_k^{∞}.

3.3 Construction of The System of Equations

The elements of the system matrix in (28) are, with the aid of (19), (24) and (26), found as

$$<e^{\infty}(\underline{\xi},w;I),\, e^{\infty}(\underline{\xi},\omega;J)>$$
$$= \int_{x\in D^T(I)} j_p(x,\omega;I) \quad \int_{y\in D^T(J)} j_q^*(y,\omega;J)F_{pq}(x,y,\omega)\mathrm{d}V, \tag{30}$$
for $I,J=1,\ldots,N$,

where

$$F_{pq}(x,y,\omega) = \int_{\underline{\xi}\in\Omega} W_{pq}(\underline{\xi},\omega)\exp[jk_0\xi_s(x_s-y_s)]\mathrm{d}\Omega \tag{31}$$

and

$$W_{pq}(\underline{\xi},\omega) = (\omega\mu_0)^2 w(\underline{\xi})(\delta_{pq}-\xi_p\xi_q). \tag{32}$$

The components of the right-hand side vector in (28) have, for the class of functions (29), the form

$$<E^{D\infty}(\underline{\xi},\omega),e^{\infty}(\underline{\xi},\omega;J)> = \int_{y\in D^T(J)} j_q^*(y,\omega;J)G_q(y,\omega)\mathrm{d}V,$$
$$\text{for } J=1,\ldots,N, \tag{33}$$

where

$$G_q(y,\omega) = \int_{\underline{\xi}\in\Omega} W_{pq}(\underline{\xi},\omega)\mathrm{A}_p^{D\infty}(\underline{\xi},\omega)\exp(-jk_0\xi_s y_s)\mathrm{d}\Omega. \tag{34}$$

Through (30) - (34) and (28) the optimization problem can be solved. In the following section several test cases, when the elements are electric dipoles, will be considered.

4 TEST ARRAYS

Our pattern synthesis method is illustrated for a number of planar arrays of ND short electric dipoles. The dipoles are taken to be uniformly oriented and non-uniformly placed in the x_1,x_2-plane. The position vector of the barycenter of the I-th dipole element is denoted by $\boldsymbol{x}(I)$, I=1,...,ND, and the uniform orientation of the electric dipoles by the unit vector $\boldsymbol{a}$. The electric current source distribution of the I-th element is taken as [28, p.29]

$$j(x,\omega;I) = a\delta[x-x(I)] \text{ for } I=1,...,ND, \tag{35}$$

where $\delta(x)$ is the three-dimensional Dirac delta function. Substitution of the source distributions (35) into (30) and (33) leads to the system of equations

$$\sum_{I=1}^{ND} c^{\text{opt}}(\omega;I)a_p a_q F_{pq}[x(I),y(J),\omega] = a_q G_q[y(J),\omega] \text{ for } J=1,...,ND. \tag{36}$$

We now take the weighting function $w(\underline{\xi})$=1. For this case, an analytical expression of the function F_{pq} in (31) can be found (see Appendix B); it is given by

$$F_{pq}(x,y,\omega) = 4\pi(\omega\mu_0)^2\left\{ \left[\delta_{pq} - \frac{(x_p-y_p)}{R}\frac{(x_q-y_q)}{R} \right] \sin(k_0R)/(k_0R) + \left[\delta_{pq} - 3\frac{(x_p-y_p)}{R}\frac{(x_q-y_q)}{R} \right] (k_0R)^{-2}[\cos(k_0R) - \sin(k_0R)/(k_0R)], \right\} \tag{37}$$

in which $R=|x-y|$. The components $a_qG_q[y(J),\omega]$, J=1,...,ND, of the right-hand side of the system of equations (36) becomes, with the choice $w(\underline{\xi})$=1,

$$a_qG_q[y(J),\omega] = (\omega\mu_0)^2\int_{\xi\in\Omega} [a_q\mathrm{A}_q^{D\infty}(\underline{\xi},\omega) - \xi_q a_q \xi_p \mathrm{A}_p^{D\infty}(\underline{\xi},\omega)] \exp[-jk_0\xi_s y_s(J)]\mathrm{d}\Omega, \text{ for } J=1,...,ND. \tag{38}$$

In this expression $A_p^{D\infty}$ is the prescribed far-field electric source current vector potential. Because the antenna configuration is symmetric with respect to the x_1,x_2-plane, a vector potential is prescribed that also reflects this symmetry and we specify its directional dependence in the halfspace $x_3>0$ only. The prescribed far-field electric source current vector potential of the whole antenna system $A_p^{D\infty}$ is taken to be linearly polarized in a constant real direction $\boldsymbol{L}$ and non-zero in a small area about the principal direction. It is taken as a function of ξ_3 through (see Fig. 2,Chapter VI, Numerical Results)

$$A_p^{D\infty}(\underline{\xi},\omega) = L_p\xi_3 H[\xi_3\text{-}\cos(\delta)] \text{ for } 0<\xi_3, \tag{39}$$

where $H(t)$ is the Heaviside unit step function defined as $H(t) = \{0,1/2,1\}$ when $\{t<0,t=0,t>0\}$ and $\delta\leq\pi/2$ is a positive constant that determines the beamwidth of the prescribed radiation pattern. Substitution of (39) into (38) leads, considering the symmetry of the integrand with respect to the x_1,x_2-plane, to

$$a_q G_q[y(J),\omega] = 2(\omega\mu_0)^2 \int_{\xi\in\Omega'} [a_q L_q - \xi_q a_q \xi_p L_p]\ \xi_3 H[\xi_3\text{-}\cos(\delta)]\exp[-jk_0\xi_s y_s(J)]d\Omega, \quad \text{for } J=1,...,ND, \tag{40}$$

where Ω' denotes the half of the unit sphere Ω located in $\xi_3>0$. Expression (40) can be determined analytically. To this end, we rewrite (40) as

$$a_q G_q[y(J),\omega] = (a_q L_q + k_0^{-2} a_q L_p \partial_q \partial_p)\text{INT}[y(J),\omega], \quad \text{for } J=1,...,ND, \tag{41}$$

where ∂_k $(k=1,2)$ denotes partial differentiation with respect to $y_k(J)$ and

$$\text{INT}[y(J),\omega] = 2(\omega\mu_0)^2 \int_{\xi\in\Omega'} \xi_3 H[\xi_3\text{-}\cos(\delta)]\exp[-jk_0\xi_s y_s(J)]d\Omega, \quad \text{for } J=1,...,ND. \tag{42}$$

The analytical evaluation of (42) leads to (see Appendix C)

$$\mathrm{INT}[y(J),\omega] = \frac{4\pi(\omega\mu_0)^2}{(k_0|y(J)|)^2} Q J_1(Q), \text{ for } J=1,\ldots,ND, \tag{43}$$

in which J_1 is the Bessel function of the first kind and of order one and its argument is given by $Q=k_0|y(J)|\sin(\delta)$. Substitution of (43) into (41) and carrying out the different partial differentiations gives us the expression for the right-hand side

$$a_q G_q[y(J),\omega] = 4\pi(\omega\mu_0)^2 \sin^2\delta \left[\frac{J_1(Q)}{Q} \left(a_p L_p - \sin^2\delta \, a_q L_p \frac{y_q(J) y_p(J)}{|y(J)|^2} \right) - \sin^2\delta \, \frac{J_2(Q)}{Q^2} \left(a_p L_p - 4 a_q L_p \frac{y_q(J) y_p(J)}{|y(J)|^2} \right) \right], \tag{44}$$

for $J=1,\ldots,ND$,

in which J_2 is the Bessel function of the first kind and of order two.

With the expressions (37) and (44) the system of equations (36) is analytically known. To fix it, the positions $x(I)$, $I=1,..ND$, and the uniform direction $\boldsymbol{a}$ of the electric dipoles have to be given and the state of polarization and beamwidth of the radiation pattern that is to be matched have to be prescribed. For some unequally-spaced arrays of electric dipole antennas numerical results will be given in the next section.

5 NUMERICAL RESULTS

For the generation and solution of the complex system of equations (36), a Fortran 77 code has been written called SYNPA (= SYNthesise of Planar Array). The input data of SYNPA are the positions and orientations of the electric dipoles and the width and the state of polarization of the prescribed beam. As output SYNPA produces several print and plot files containing the chosen antenna configuration (plot), the computed complex excitations (print), the global error

$$\mathrm{NERR}=\mathrm{ERR}/\|E^{D\infty}\| \tag{45}$$

(print), where ERR is defined in (20) and $\|E^{D\infty}\|$ is the norm of the described radiation pattern, and the corresponding radiation pattern (plots). From the synthesized radiation field 2D-plots of the *H*-, *D*-, and *E*-plane as well as a 3D-plot are given. Additional Fortran 77 codes have been written that have these plot files as input and produce screen and hardcopy output. These codes make use of the subroutines from the UNIRAS library [29]. As an additional option, one can carry out the synthesis for digitized complex excitations. This option is of interest when we have to deal with n-bits amplifiers and m-bits phase shifters.

For the evaluation of the right-hand side of the system of equations (36) SYNPA makes use of the Bessel functions from the IMSL Library [30]. For the solution of (36) SYNPA uses the conjugate gradient method presented in [31] without any preconditioning. SYNPA has been implemented on a Vax 6310 computer and computation times needed for the numerical examples given in this section are in the order of seconds.

The synthesis problem is illustrated for a number of square, planar arrays of 9x9 electric dipoles. For each array, the center element is taken to be at the origin O of the reference frame (phase center of the antenna) and the elements are arranged such that they are parallel to the coordinate axes. The currents in the electric dipoles flow parallel to the x_1-direction. The (non-uniform) arrangements of the elements in the x_1- and x_2-directions are chosen to be identical and in such a way that the array configuration is symmetric with respect to the two coordinate axes. (see Fig. 1). The element rows parallel to the x_1-axis are numbered as -4, -3, ..., 3, 4, where row 0 is the one that coincides with this axis. The spacing between rows i and j is denoted by s_{ij} and is expressed in terms of wavelengths. By specifying s_{01}, s_{12}, s_{23} and s_{34}, the element spacings of the whole array are fixed. (see Fig. 1). The numerical experiments are carried out for the four arrays defined in Table I.

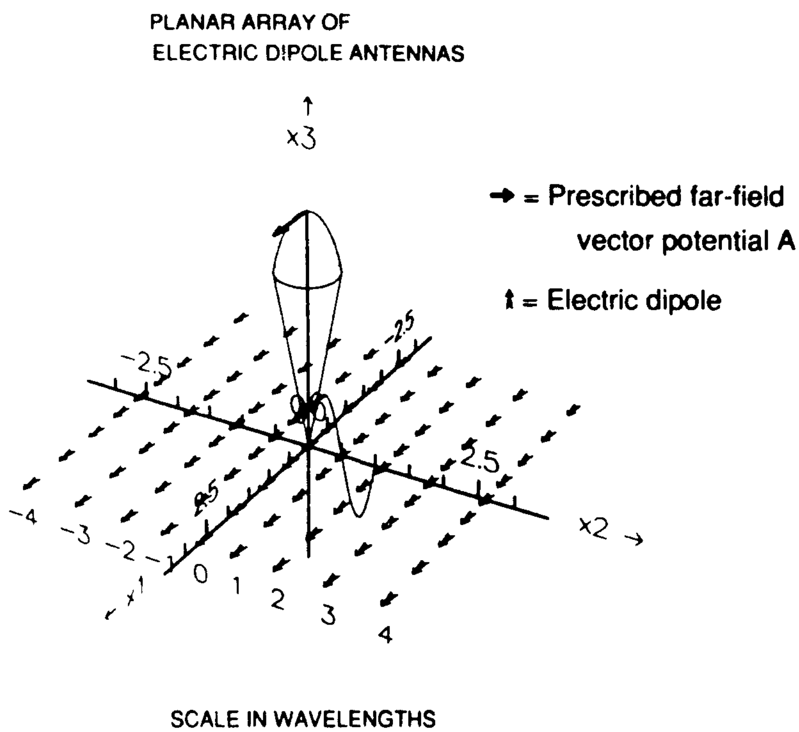

Fig. 1: The square planar array antenna of 9x9 unequally spaced electric dipoles. The prescribed vector potential *A* is shown from which the prescribed electric field *E* follows.

Results for grids I-IV							
Grid	s_{01} (λ)	s_{12} (λ)	s_{23} (λ)	s_{34} (λ)	Type of grid	Number of iterations	NERR (%)
I	0.5	0.5	0.5	0.5	equispaced	23	39
II	0.3	0.3	0.3	0.3	equispaced	57	43
III	0.5	0.6	0.7	0.8	unequally spaced	20	37
IV	0.5	0.75	1.0	1.25	unequally spaced	19	46

Table I: The four different grids with their spacings s_{01}, s_{12}, s_{23} and s_{34}. The number of iterations needed for the solution of the corresponding system of equations for each grid and the related computed normalized mean square error NERR are shown.

The radiation pattern that has to be approximated is prescribed via the far-field electric source current distribution $A_r^{D\infty}$ (cf. (29), see Fig. 1). We choose the direction of this vector in the positive x_1-direction. Its angular dependence is given by (39) in which we choose $\delta = 15°$, i.e. the prescribed beamwidth is 30°. In Fig. 2 the prescribed radiation field is presented.

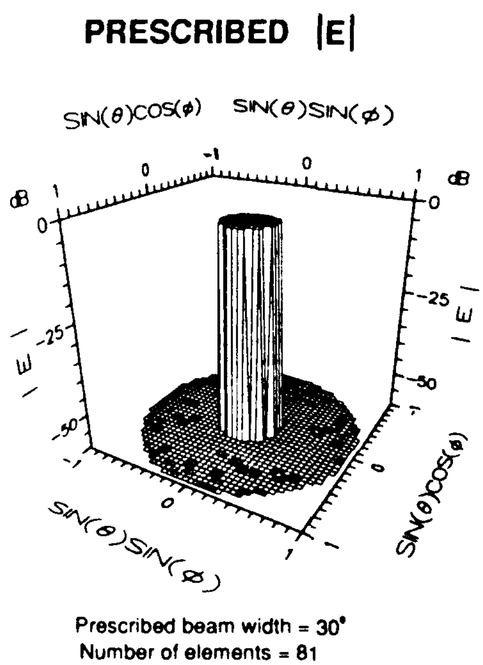

Fig. 2: The prescribed radiation pattern of beamwidth 30°.

The results of the synthesis for the four planar arrays are given in Table 1 and Figs. 3-10. In Table 1 the number of iteration steps needed for the solution of the system of equations for each of the four grids are given. A large number of iteration steps suggests a poor condition of the system matrix. Further, in Table I the normalized global mean square error NERR is given which is a measure of the accuracy of approximation. In Figs. 3-6 three-dimensional plots of the synthesized radiation fields are shown and in Figs. 7-10 the two-dimensional plots of the prescribed and synthesized radiation fields in the H-, D- and E-planes are shown.

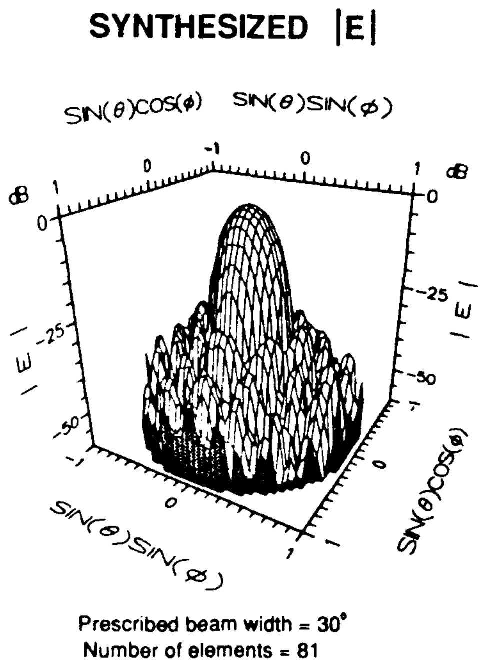

Fig. 3: The synthesized total radiation pattern corresponding to grid I.

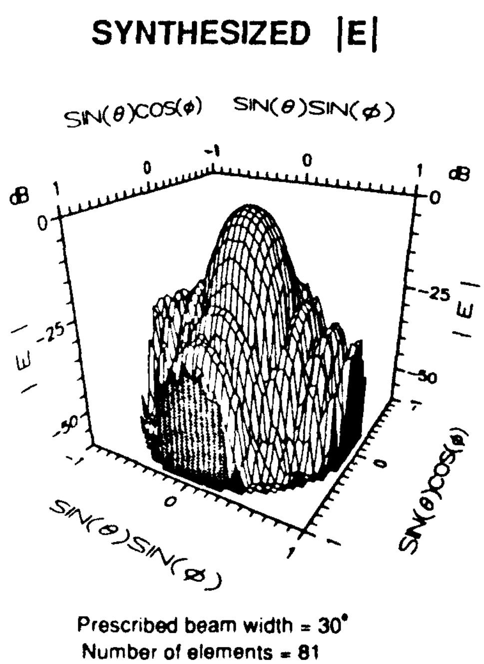

Fig. 4: The synthesized total radiation pattern corresponding to grid II.

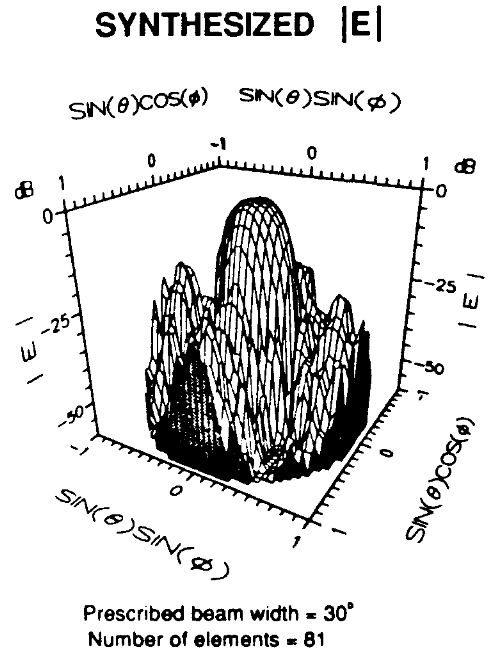

Fig. 5: The synthesized total radiation pattern corresponding to grid III.

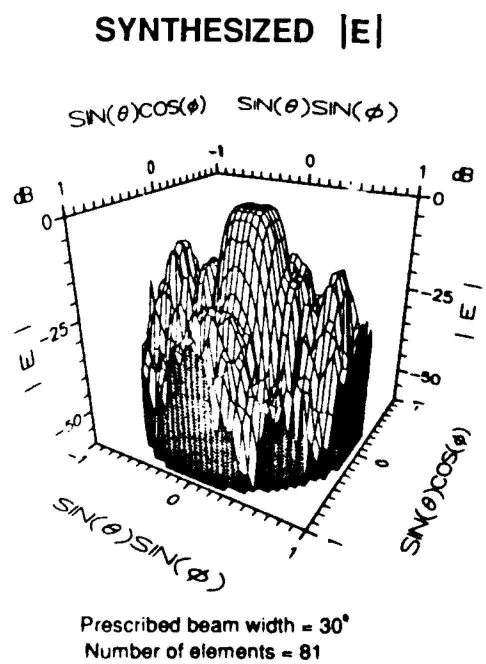

Fig. 6: The synthesized total radiation pattern corresponding to grid IV.

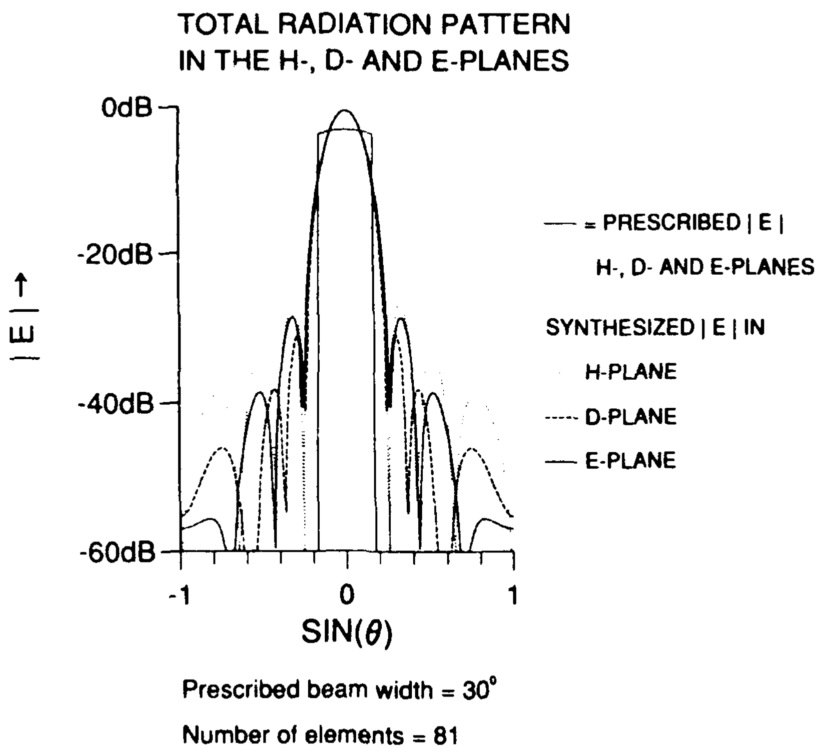

Fig. 7: The total radiation pattern in *H*-, *D*- and *E*-planes of the prescribed and synthesized radiation field corresponding to grid I.

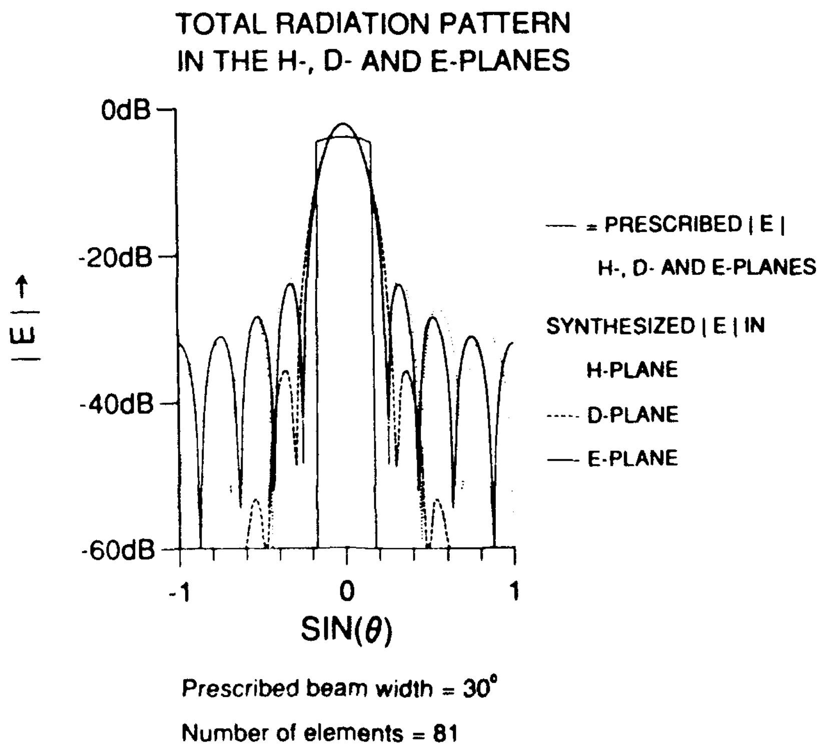

Fig. 8: The total radiation pattern in *H*-, *D*- and *E*-planes of the prescribed and synthesized radiation field corresponding to grid II.

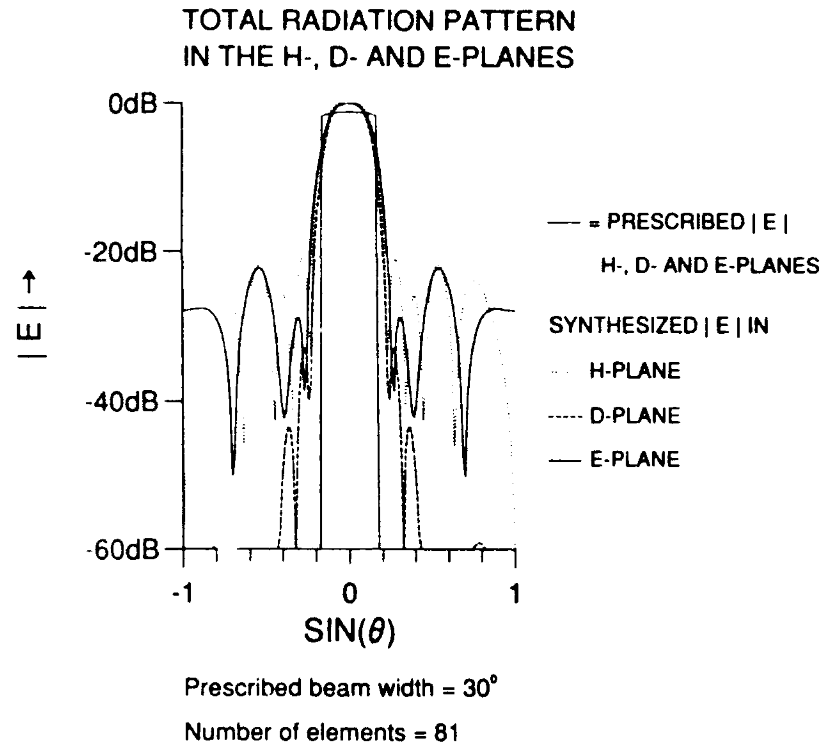

Fig. 9: The total radiation pattern in *H*-, *D*- and *E*-planes of the prescribed and synthesized radiation field corresponding to grid III.

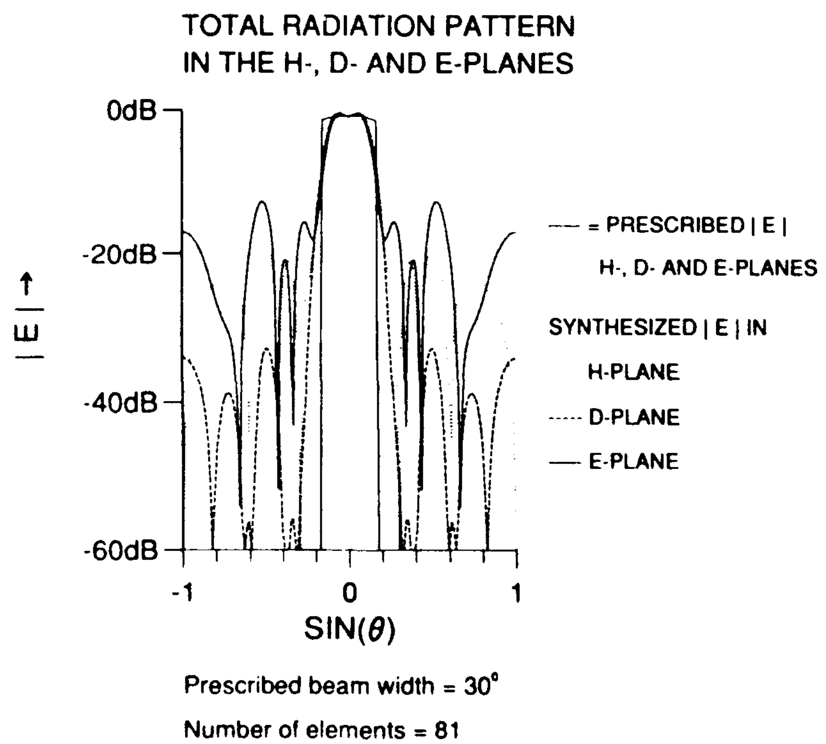

Fig. 10: The total radiation pattern in *H*-, *D*- and *E*-planes of the prescribed and synthesized radiation field corresponding to grid IV.

Grids I and II are in fact identical grids that are excited at different frequencies. For grid I with its 0.5 wavelength interelement spacing we have a higher frequency of excitation than for grid II with its 0.3 wavelength interelement spacing. From Table 1 we learn that the global error NERR for the synthesis for grid II is larger than the one for grid I. Further, the plots of Figs. 3-4 and Figs. 7-8 show that the sidelobes of the synthesized pattern for grid II are higher than the ones for grid I. Finally, the number of iterations needed for the solution of the system of equations for grid II is larger than the one for grid I. Apparently the condition of the system matrix in the former case is poorer.

The experiments for grid III and IV are the ones for unequally-spaced arrays. The results for grid III show a lower global error NERR than the ones obtained for the equally-spaced grids I and II. The sidelobes of the synthesized radiation pattern for grid III are higher than the ones for grid I and II but the approximation of the main beam is better than for the grids I and II (see Fig. 9). In grid IV we have unequally-spaced electric dipoles with larger interspacings than for grid III. For this case the main beam is even better approximated (Fig. 6 and Fig. 10). However, the sidelobe level is much higher than for grid III and gives rise to a global error NERR that is higher than for the case with grid III.

Although Figs. 3-10 show that for the four experiments we have a good approximation of the prescribed radiation pattern we found rather large global errors NERR in the order of 40%. These large errors are mainly due to the presence of the steep slopes of the prescribed beam. A prescribed beam with less steep slopes and the same beamwidth will result into a significantly smaller NERR. However, for such a prescribed radiation pattern the right-hand side of the system of equations cannot be evaluated analytically and a numerical evaluation of the resulting integrals is required (which can easily be carried out).

Next, the pattern matching is carried out for grid I (see Table 1) for the case that the elements are excited with 2-bits amplitude excitations. (The number of bits of the phase excitations is not important because the optimal solution implies zero phases impressed on the dipole antennas). This solution for digitized excitations is derived from the solution for "continuous" excitations by taking the digitized excitations that are closest to the "continuous excitations". Fig. 11 shows the 3D-plot of the synthesized radiation pattern with digitized excitations and Figs. 12-14 shows the total radiation field in the *H*-, *D*- and *E*-planes for both the digitized and the "continuous" excitations.

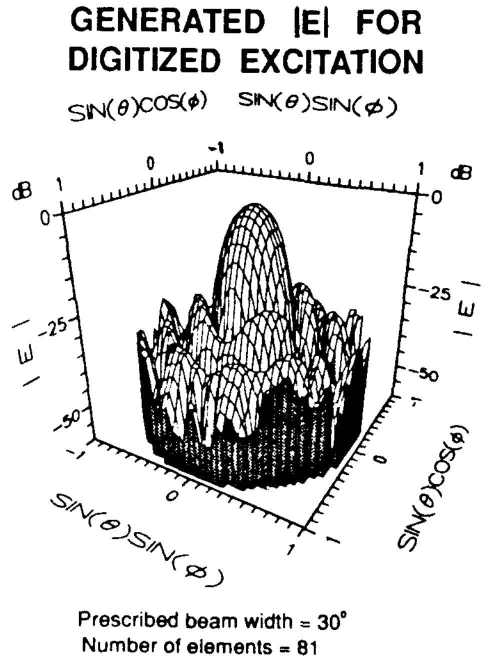

Fig. 11: The synthesized total radiation pattern corresponding to grid I for the case of 2-bits amplitude excitations.

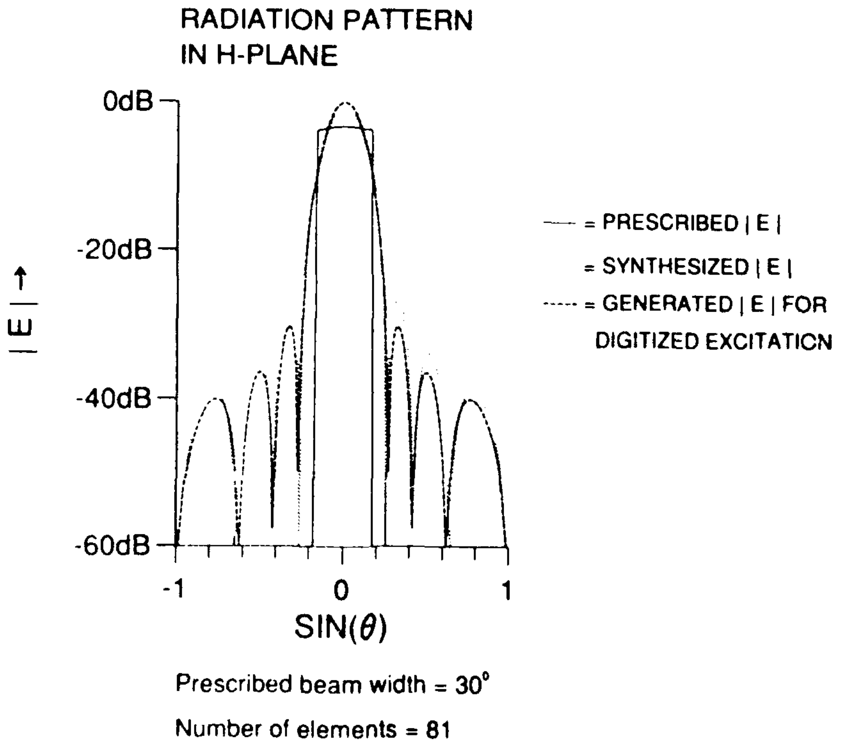

Fig. 12: The total radiation pattern in H-plane of the prescribed, digitized and "continuous" synthesized radiation field corresponding to grid I for the case of 2-bits amplitude excitations.

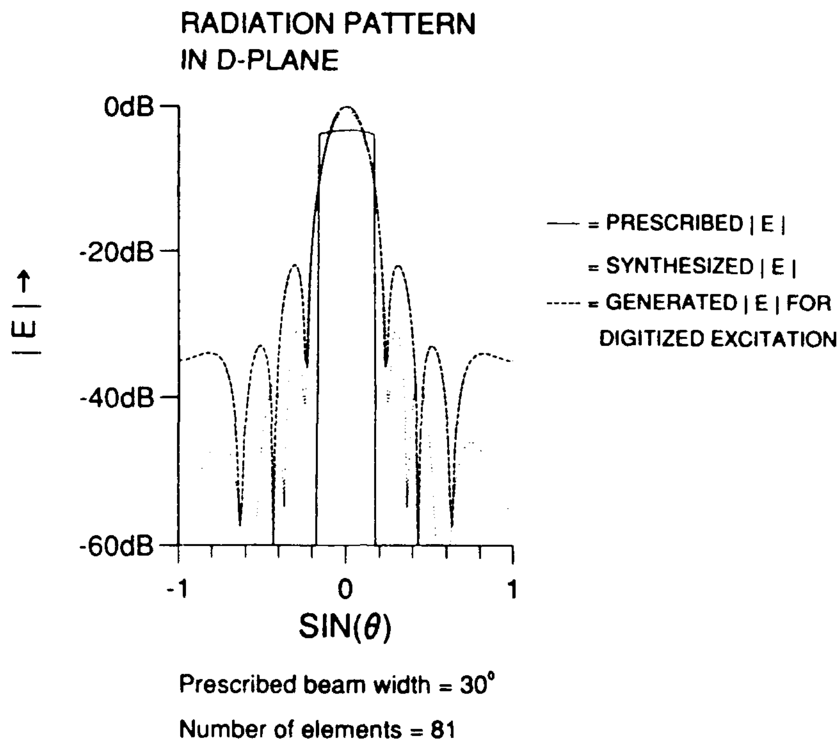

Fig. 13: The total radiation pattern in *D*-plane of the prescribed, digitized and "continuous" synthesized radiation field corresponding to grid I for the case of 2-bits amplitude excitations.

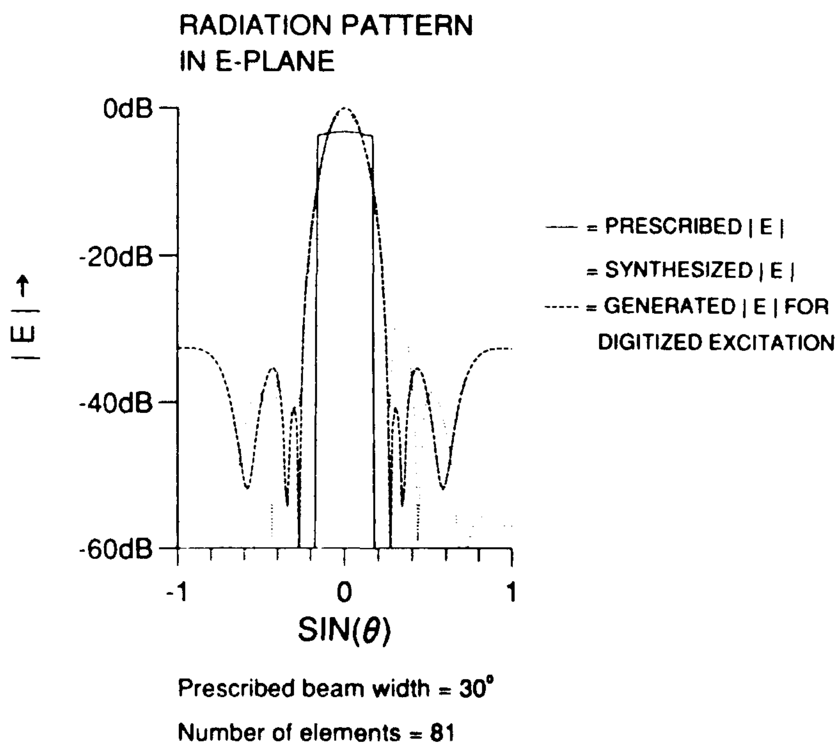

Fig. 14: The total radiation pattern in *E*-plane of the prescribed, digitized and "continuous" synthesized radiation field corresponding to grid I for the case of 2-bits amplitude excitations.

From these plots we see that for the case of the digitized amplitude excitations the approximation of the main beam is nearly as accurate as for the continuous case while the sidelobes of the radiation pattern for the digitized amplitude excitations are higher than the ones for the continuous case. For the digitized case we find NERR=42% which is slightly higher than the value of NERR for the continuous case.

6 CONCLUSION

A novel method of array antenna pattern synthesis is presented that is based on an optimization technique. The complex excitation values of the current distributions of the array elements are taken as parameters. The radiated far-field pattern is matched to one that is prescribed by minimizing a global mean-square error. The method is applicable to arrays with unequally-spaced, non-identical elements (for which a factorization of the radiation pattern into an element factor and an array factor is impossible). Numerical experiments show the feasibility of the method.

REFERENCES

[1] M. T. Ma,
Theory and Application of Antenna Arrays.
New York: Wiley, 1974.

[2] D. K. Cheng,
"Optimization Techniques for Antenna Arrays,"
in *Proc. IEEE*, vol. 59, no. 12, pp. 23-33, December 1971.

[3] M. S. Shashikant and J. K. Butler,
"Constrained optimization of the performance indices of arbitrary array antennas,"
IEEE Trans. Antennas Propagat., vol. AP-19, pp. 493-498, Jul. 1971.

[4] H. Steyskal,
"Synthesis of antenna patterns with prescribed nulls,"
IEEE Trans Antennas Propagat., vol. AP-30, pp. 273-279, Mar. 1982.

[5] S. R. Laxpati,
"Planar array synthesis with prescribed nulls,"
IEEE Trans. Antennas Propagat., vol. AP-30, pp. 1176-1183, Nov. 1982.

[6] K. Hirasawa,
"The application of a biquadratic programming method to phase-only optimization of antenna arrays,"
IEEE Trans. Antennas Propagat., vol. 36, pp. 1545-1550, Nov. 1988.

[7] P. M. Woodward and J. D. Lawson,
"The theoretical precision with which an arbitrary radiation-pattern may be obtained from a source of finite size,"
J. IEE, pp. 363-373, Mar. `1948.

[8] W. L. Stutzman,
"Synthesis of shaped-beam radiation patterns using the iterative sampling method,"
IEEE Trans. Antennas Propagat., vol. AP-19, pp. 36-41, Jan. 1971.

[9] W. L. Stutzman,
"Radiation pattern synthesis of planar antennas using the iterative sampling method,"
IEEE Trans. Antennas Propagat., vol. AP-23, pp. 764-769, Nov. 1975.

[10] H. Schjaer-Jacobsen and K. Madsen,
"Synthesis of nonuniformly spaced arrays using a general minimax optimization method,"
IEEE Trans. Antennas Propagat., vol. AP-24, pp. 501-506, July 1976.

[11] R. S. Elliott and G. J. Stern,
"A new technique for shaped beam synthesis of equispaced arrays,"
IEEE Trans. Antennas Propagat., vol. AP-32, pp. 1129-1133, Oct. 1984.

[12] H. J. Orchard, R. S. Elliott, and G. J. Stern,
"Optimising the synthesis of shaped beam antenna patterns,"
IEE Proceedings, vol. 132, Pt. H, pp. 63-68, Feb. 1985.

[13] R. Streit.
"Sufficient conditions for the existence of optimum beam patterns for unequally spaced linear arrays with an example,"
IEEE Trans. Antennas Propagat., vol. AP-23, pp. 112-115, Jan. 1975.

[14] A. C. Schell and A. Ishimaru,
"Antenna Pattern Synthesis,"
in *Antenna Theory*, R. E. Collin and F. J. Zucker, Eds..
New York: McGraw-Hill, 1969, part I.

[15] J. R. Mautz and R. F. Harrington,
"Computational methods for antenna pattern synthesis,"
IEEE Trans. Antennas Propagat., vol. AP-23, pp. 507-512, Jul. 1975

[16] G. Franceschetti, G. Mazzarella, and G. Panariello,
"Array synthesis with excitation constraints,"
IEE Proceedings, vol. 135, Pt. H, pp. 400-407, Dec. 1988.

[17] H. Elmikati and A. A. Elsohly,
"Extension of projection method to nonuniformly linear antenna arrays,"
IEEE Trans. Antennas Propagat., vol. AP-32, pp. 507-512, May 1984.

[18] G. T. Poulton,
"Antenna power pattern synthesis using method of successive projections,"
Electronics Letters, vol. 22, pp. 1042-1043, Sept. 1986.

[19] O. M. Bucci, G. Franceschetti, G. Mazarella, and G. Panariello,
"Intersection approach to array pattern synthesis,"
IEE Proceedings, vol. 137, Pt. H, pp. 349-357, Dec. 1990.

[20] H. Unz,
"Linear arrays with arbitrarily distributed elements,"
IRE Trans. Antennas Propagat., vol. AP-8, pp. 222-223, Mar. 1960.

[21] D. D. King, R. F. Packard, and R. K. Thomas,
"Unequally-spaced, broad-band antenna arrays,"
IRE Trans. Antennas Propagat., vol. AP-8, pp. 380-385, July 1960.

[22] M. G. Andreasen,
"Linear arrays with variable interelement spacings,"
IRE Trans. Antennas Propagat., vol. AP-10, pp. 137-143, Mar. 1962.

[23] R. E. Wiley,
"Space tapering of linear and planar arrays,"
IRE Trans. Antennas Propagat., vol. AP-10, Jul. 1962.

[24] A. Ishimaru,
"Theory of unequally-spaced arrays,"
IRE Trans. Antennas Propagat., vol. AP-10, pp. 691-702, Nov. 1962.

[25] M. I. Skolnik, G. Nemhauser, and J. W. Sherman III,
"Dynamic programming applied to unequally-spaced arrays,"
IEEE Trans. Antennas Propagat., vol AP-12, pp. 35-43, Jan. 1964.

[26] A. Ishimaru and Y. S. Chen,
"Thinning and broadbanding antenna arrays by unequal spacings,"
IEEE Trans. Antennas Propagat., vol. AP-13, pp. 34-42, Jan. 1965.

[27] Y. T. Lo and S. W. Lee,
"A study of space-tapered arrays,"
vol. AP-14, pp. 22-30, Jan. 1966

[28] R. E. Collin and F. J. Zucker,
Antenna Theory.
New York: McGraw Hill, 1969, part I.

[29] UNIRAS A/S Soborg, Denmark, 1988.

[30] IMSL, SFUN/LIBRARY, version 2.1, Houston, IMSL, 1989, subroutine BSJNS.

[31] P. M. van den Berg,
"Iterative schemes based on minimization of a uniform error criterion,"
in *Progress in Electromagnetics Research*, vol. 5, *Application of Conjugate Gradient Method to Electromagnetics and Signal Analysis*,
T. K. Sarkar, Ed., New York: Elsevier Science Publishing Co., 1991, Chapter 2.

[32] M. Abramowitz and I. A. Stegun,
Handbook of Mathematical Functions.
New York: Dover Publications, 1965.

G.A. van der Spek
(group leader)

J.G. van Hezewijk
(project leader)

DERIVATION OF CONDITION FOR OPTIMUM EXCITATION

In this appendix the condition for the optimum excitations $c^{opt}(\omega;I)$, $I=1,\dots,N$, is derived from Equation (27). To this end, the variational analysis presented in [31] is applied. We put

$$c(\omega;I) = c^{opt}(\omega;I) + \delta c(\omega;I) \text{ for } I=1,\dots,N, \tag{A1}$$

where $\delta c(\omega;I)$ is an arbitrary deviation from $c^{opt}(\omega;I)$. Substitution of (A1) into (27) leads to

$$\begin{aligned}
\|E^{\infty}-E^{D\infty}\|_{\Omega}^2 &= \|E^{D\infty}\|_{\Omega}^2 - 2\mathrm{Re}\{\sum_{I=1}^{N}[c^{opt*}(\omega;I)+\delta c^*(\omega;I)]<E^{D\infty}(\underline{\xi},\omega),e^{\infty}(\underline{\xi},\omega;I)>\} \\
&+ \sum_{I=1}^{N}\sum_{J=1}^{N}[c^{opt}(\omega;I)+\delta c(\omega;I)][c^{opt*}(\omega;J)+\delta c^*(\omega;J)] <e^{\infty}(\underline{\xi},\omega;I),e^{\infty}(\underline{\xi},\omega;J)> \\
&= \mathrm{ERR}^2(E^{\infty opt}) + 2\mathrm{Re}\Bigg[\sum_{J=1}^{N}\delta c^*(\omega;J) \\
&\left(\sum_{I=1}^{N}c^{opt}(\omega;I)<e^{\infty}(\underline{\xi},\omega;I),e^{\infty}(\underline{\xi},\omega;J)> - <E^{D\infty}(\underline{\xi},\omega),e^{\infty}(\underline{\xi},\omega;J)>\right)\Bigg] \\
&+ \sum_{I=1}^{N}\sum_{J=1}^{N}\delta c(\omega;I)\delta c^*(\omega;J)<e^{\infty}(\underline{\xi},\omega;I),e^{\infty}(\underline{\xi},\omega;J)>.
\end{aligned} \tag{A2}$$

For $c^{opt}(\omega;I)$, $I=1,\dots,N$, to be a minimum of ERR (i.e., we have a minimum for $\delta c(\omega;I)=0$, $I=1,\dots,N$), the terms in (A2) that are linear in $\delta c^*(\omega;J)$ have to compensate each other. This leads to the condition

$$\sum_{I=1}^{N}c^{opt}(\omega;I)<e^{\infty}(\underline{\xi},\omega;I),e^{\infty}(\underline{\xi},\omega;J)> = <E^{D\infty}(\underline{\xi},\omega),e^{\infty}(\underline{\xi},\omega;J)> \quad \text{for } J=1,\dots,N. \tag{A3}$$

DERIVATION OF EXPLICIT EXPRESSION FOR F_{pq}

In this appendix the explicit expression for $F_{pq}(x,y,\omega)$ in the case of a constant weighting function $w(\underline{\underline{\xi}})=1$ is derived. From (31) and (32) we then have

$$F_{pq}(x,y,\omega) = \int_{\underline{\underline{\xi}}\in\Omega} (\omega\mu_0)^2(\delta_{pq}-\xi_p\xi_q)\exp(jk_0\xi_s r_s)\mathrm{d}\Omega, \qquad \text{(B1)}$$

in which $r_s=x_s-y_s$. Integration of the first term T1 in (B1) gives

$$\mathrm{T1} = (\omega\mu_0)^2\delta_{pq} \int_{\xi\in\Omega} \exp(jk_0\xi_s r_s)\mathrm{d}\Omega = 4\pi(\omega\mu_0)^2\delta_{pq}\sin(k_0R)/(k_0\mathrm{R}), \qquad \text{(B2)}$$

where $R=|r|$. The integration of the second term T2 is found by using

$$\mathrm{T2} = -(\omega\mu_0)^2 \int_{\underline{\underline{\xi}}\in\Omega} \xi_p\xi_q\exp(jk_0\xi_s r_s)\mathrm{d}\Omega = [(\omega\mu_0)^2/k_0^2]\partial_p\partial_q \int_{\underline{\underline{\xi}}\in\Omega} \exp(jk_0\xi_s r_s)\mathrm{d}\Omega, \qquad \text{(B3)}$$

where ∂_p denotes partial differentiation with respect to r_p. Using the results of (B2) into (B3) leads to

$$\begin{aligned} \mathrm{T2} &= 4\pi[(\omega\mu_0)^2/k_0^2]\partial_p\partial_q[\sin(k_0R)/(k_0\mathrm{R})] \\ &= 4\pi[(\omega\mu_0)^2/(k_0R)^2] \left\{ \delta_{pq}[\cos(k_0R) - \sin(k_0R)/(k_0\mathrm{R})] \right. \\ &\left. - \frac{r_p r_q}{R^2} \{3[\cos(k_0R) - \sin(k_0R)/(k_0R)] + (k_0R)\sin(k_0R)\} \right\}. \end{aligned} \qquad \text{(B4)}$$

Summing the two terms T1 and T2 gives for (B1)

$$F_{pq}(x,y,\omega) = 4\pi(\omega\mu_0)^2 \left\{ \left[\delta_{pq} - \frac{r_p r_q}{R^2} \right] \sin(k_0R)/(k_0R) \right.$$

$$\left. + \left[\delta_{pq} - 3\,\frac{r_p r_q}{R^2} \right] (k_0R)^{-2}[\cos(k_0R) - \sin(k_0R)/(k_0R)] \right\}. \quad \text{(B5)}$$

For the case $r=0$ ($x=y$) the expression for F_{pq} can be found by taking the limit $R \to 0$ in (B5). A more straightforeward manner is the substitution of $r=0$ in formula (B1) which entails that the exponential function becomes one, and hence

$$F_{pq}(x,x,\omega) = \int_{\xi \in \Omega} (\omega\mu_0)^2(\delta_{pq} - \xi_p\xi_q)\mathrm{d}\Omega. \quad \text{(B6)}$$

For the determination of (B6) we introduce spherical coordinates θ and ϕ, where θ is the angle between $\underline{\xi}$ and the positive x_3-axis and ϕ the angle that the projection of $\underline{\xi}$ on the x_1,x_2-plane makes with the positive x_1-axis. In terms of these coordinates, the unit vector in the direction of observation $\underline{\xi}$ is

$$\underline{\xi} = [\sin(\theta)\cos(\phi), \sin(\theta)\sin(\phi), \cos(\theta)]^T, \quad \text{(B7)}$$

and the Jacobian is $\sin(\theta)$. Substitution of (B7) into (B6) gives for the expressions of (B6) for which $p=q$:

$$F_{11}(x,x,\omega) = (\omega\mu_0)^2 \int_{\phi=0}^{2\pi} \mathrm{d}\phi \int_{\theta=0}^{\pi} [1-\sin^2(\theta)\cos^2(\phi)]\sin(\theta)\mathrm{d}\theta = (8/3)\pi(\omega\mu_0)^2, \quad \text{(B8)}$$

$$F_{22}(x,x,\omega) = (\omega\mu_0)^2 \int_{\phi=0}^{2\pi} \mathrm{d}\phi \int_{\theta=0}^{\pi} [1-\sin^2(\theta)\sin^2(\phi)]\sin(\theta)\mathrm{d}\theta = (8/3)\pi(\omega\mu_0)^2, \quad \text{(B9)}$$

and

$$F_{33}(x,x,\omega) = (\omega\mu_0)^2 \int_{\phi=0}^{2\pi} d\phi \int_{\theta=0}^{\pi} [1-\cos^2(\theta)]\sin(\theta)d\theta = (8/3)\pi(\omega\mu_0)^2 \qquad \text{(B10)}$$

For the case that $p \neq q$ the components of the expression in (B6) are zero. Combining the results (B8)-(B10) we find

$$F_{pq}(x,y,\omega) = (8/3)\pi(\omega\mu_0)^2\delta_{pq}. \qquad \text{(B11)}$$

ANALYTICAL EVALUATION OF INTEGRAL

In this Appendix we perform the analytical evaluation of integral (42)

$$\mathrm{INT}[y(J),\omega] = 2(\omega\mu_0)^2 \int_{\underline{\underline{\xi}}\in\Omega'} \xi_3\{H[\xi_3-\cos(\delta)]\}\exp[-jk_0\xi_s y_s(J)]\mathrm{d}\Omega, \quad \text{for } J=1,\ldots,ND. \tag{C1}$$

For the determination of (C1) we introduce spherical coordinates θ and ϕ, where θ is the angle between $\underline{\underline{\xi}}$ and the positive x_3-axis and ϕ the angle that the projection of $\underline{\underline{\xi}}$ on the x_1,x_2-plane makes with the vector $y(J)$. This choice with respect to the angle ϕ leads to a simple expression for the inner product in the exponent of the exponential function. In terms of these coordinates, the unit vector in the direction of observation $\underline{\underline{\xi}}$ is

$$\underline{\underline{\xi}} = [\sin(\theta)\cos(\phi),\sin(\theta)\sin(\phi),\cos(\theta)]^{\mathrm{T}}, \tag{C2}$$

the Jacobian is $\sin(\theta)$ and for the inner product we find

$$\xi_s y_s(J)=|y(J)|\sin(\theta)\cos(\phi). \tag{C3}$$

Substitution of (C2) and (C3) into (C1) gives

$$\mathrm{INT}[y(J),\omega] = 2(\omega\mu_0)^2 \int_{\phi=0}^{2\pi} \mathrm{d}\phi \int_{\theta=0}^{\pi/2} \cos(\theta)\{H[\cos(\theta)-\cos(\delta)]\} \exp[-jk_0|y(J)|\sin(\theta)\cos(\phi)]\sin(\theta)\mathrm{d}\theta, \text{ for } J=1,\ldots,ND. \tag{C4}$$

Equation (C4) is rewritten as

$$\mathrm{INT}[y(J),\omega] = 4(\omega\mu_0)^2 \int_{\theta=0}^{\delta} \sin(\theta)\cos(\theta)\mathrm{d}\theta \int_{\phi=0}^{\pi} \exp[-jk_0|y(J)|\sin(\theta)\cos(\phi)]\mathrm{d}\phi. \tag{C5}$$

Using the theory of Bessel functions (see [32]) the integration with respect to ø leads to

$$\mathrm{INT}[y(J),\omega] = 4\pi(\omega\mu_0)^2 \int_{\theta=0}^{\delta} \sin(\theta)\cos(\theta) J_0[k_0|y(J)|\sin(\theta)]\,d\theta, \tag{C6}$$

for $J=1,\ldots,ND$.

in which J_0 is the Bessel function of the first kind and of order zero. Next, using the property (see [32])

$$tJ_0(t) = \frac{d}{dt}[tJ_1(t)] \tag{C7}$$

we find

$$\mathrm{INT}[y(J),\omega] = \frac{4\pi(\omega\mu_0)^2 Q J_1(Q)}{(k_0|y(J)|)^2}, \text{ for } J=1,\ldots,ND \tag{C8}$$

where J_1 is the Bessel function of the first kind of order one and $Q=k_0|y(J)|\sin(\delta)$.

REPORT DOCUMENTATION PAGE (MOD-NL)

1. DEFENSE REPORT NUMBER (MOD-NL) TD91-3694	2. RECIPIENT'S ACCESSION NUMBER —	3. PERFORMING ORGANIZATION REPORT NUMBER FEL-91-A305
4. PROJECT/TASK/WORK UNIT NO. 22231	5. CONTRACT NUMBER A91KM636	6. REPORT DATE NOVEMBER 1991
7. NUMBER OF PAGES 39 (INCL. 3 APPENDICES, EXCL. RDP & DISTRIBUTION LIST)	8. NUMBER OF REFERENCES 32	9. TYPE OF REPORT AND DATES COVERED FINAL REPORT

10. TITLE AND SUBTITLE
PATTERN SYNTHESIS FOR UNEQUALLY-SPACED ARRAY ANTENNAS WITH NON-IDENTICAL ELEMENTS

11. AUTHOR(S)
H.J. STAM

12. PERFORMING ORGANIZATION NAME(S) AND ADDRESS(ES)
TNO PHYSICS AND ELECTRONICS LABORATORY, P.O. BOX 96864, 2509 JG THE HAGUE
OUDE WAALSDORPERWEG 63, THE HAGUE, THE NETHERLANDS

13. SPONSORING/MONITORING AGENCY NAME(S)
ADMIRALITEIT KONINKLIJKE MARINE

14. SUPPLEMENTARY NOTES

15. ABSTRACT (MAXIMUM 200 WORDS, 1044 POSITIONS)
A NOVEL METHOD OF ARRAY ANTENNA PATTERN SYNTHESIS IS PRESENTED THAT IS BASED ON AN OPTIMIZATION TECHNIQUE. THE COMPLEX EXCITATION VALUES OF THE CURRENT DISTRIBUTION OF THE ARRAY ELEMENTS ARE TAKEN AS PARAMETERS. THE RADIATED FAR FIELD PATTERN IS MATCHED TO ONE THAT IS PRESCRIBED BY MINIMIZING A GLOBAL MEAN SQUARE ERROR. THE METHOD IS SUITABLE FOR GENERAL ARRAYS LIKE LINEAR, PLANAR AND CONFORMAL ONES, AND DOES NOT REQUIRE THE FACTORIZATION INTO AN ELEMENT FACTOR AND AN ARRAY FACTOR. IN CONTRAST WITH FOURIER-LIKE METHODS THE ARRAY ELEMENTS MAY BE ARBITRARILY PLACED. ALTHOUGH THE THEORY IS DEVELOPED FOR ARRAYS OF IDENTICAL ELEMENTS, IT APPLIES TO THE CASE OF ARRAYS CONTAINING NON-IDENTICAL ELEMENTS AS WELL. NUMERICAL RESULTS ARE PRESENTED FOR UNEQUALLY-SPACED PLANAR ARRAYS OF SHORT ELECTRIC DIPOLES.

16. DESCRIPTORS ANTENNA RADIATION PATTERNS ANTENNA ARRAYS PLANAR ANTENNA ARRAY	IDENTIFIERS PATTERN SYNTHESIS

17a. SECURITY CLASSIFICATION (OF REPORT) UNCLASSIFIED	17b. SECURITY CLASSIFICATION (OF PAGE) UNCLASSIFIED	17c. SECURITY CLASSIFICATION (OF ABSTRACT) UNCLASSIFIED
18. DISTRIBUTION/AVAILABILITY STATEMENT UNLIMITED DISTRIBUTION		17d. SECURITY CLASSIFICATION (OF TITLES) UNCLASSIFIED